ORAL 09

Development of Micro-scale CFD Model to Predict Wind Environment on Complex Terrain

Taehwan Ha* and In-bok Lee

Department of Rural Systems Engineering, Research Institute for Agriculture and Life Sciences, College of Agriculture and Life Sciences, Seoul National University, 599, Gwanakno, Gwanakgu, Seoul 151-921, Republic of Korea

I. Introduction

Over 65% of South Korea's land is covered in forests. Atmospheric from mountainous area shows different phenomena compared to the atmospheric from flat area due to dynamic change of topography and altitude and airflow resistance of forest. Korea government has constructed 128 mountain meteorological observation systems in order to provide more accurate mountain weather to people and to predict mountain disaster such as a fire, a landslide, dispersion of pollutant and so on. Although the number of mountain meteorological observation system is increasing, it is not enough compared to the number of flat area weather station. The method of meteorological observation of South Korea was revised on 2012, however there is no standard for installation of the mountain meteorological observation system located in forest. World Meteorological Organization (WMO) recommended that weather observation system in forest should be located in clear-cutting, and the distance to obstacle from the system should be more than 20 times its maximum height (World Meteorological Organization, 2008).

However, study for appropriate size of clear-cut is need because of the recommended size of clear-cut was too wide. The proper clear-cut size could be analysed by field experiment or Computational Fluid Dynamics (CFD). However, field experiment has some experimental limitations: 1) difficulties in acquiring results due to unstable and unpredictable environmental conditions; 2) difficulties in changing the experimental condition such as size of clear-cutting; 3) time- and labor- consuming problems. Otherwise, numerical simulation such as Computational Fluid Dynamics (CFD) has some strengths: 1) it can analyze result according to various experimental condition with low cost; 2) it can repeat experiment easily with low cost and short time; 3) it can predict and visualize air flow pattern (Cheng and Hu, 2005; Hong *et al*., 2011; Kim and Baik, 1999; Kim and Baik, 2001; Liu and Barth, 2002; Sini *et al.*, 1996). Because of the strengths, CFD has increasingly been used to simulate microscale wind environment near the surface considering the obstacle with small grid size in complex and mountainous terrain.

The aim of this study is development of micro-scale CFD model to predict micro climate over complex terrain, because analysis of micro-climate is essential to estimate proper clear-cut size to

* Correspondence to : iblee@snu.ac.kr

install weather observation system in forest.

II. Materials and Methods

2.1. Target site

The target site for development was Gwangneung arboretum located in Pocheon-si, Gyeonggi-do, South Korea where two flux towers were constructed in 2006 and 2007, respectively. The target area consisted of various land cover types, and surface of the target area was classified into 13 zones based on land cover classification category of National Geographic Information Institute of South Korea. The classified 13 lane usages were categorized as forest and non-forest region, and the forest region consisted of conifer forest and deciduous forest. Elevation range of the target area was about from 75 m to 535 m and valley was formed in an east-west direction.

Fig. 1. Satellite image of target area (left) and land use classification of target area (right).

Conifer trees and deciduous trees were distributed around the GCK flux tower and GDK flux tower, respectively, and its characteristics are shown in Table 1. The elevation of GCK flux tower(37° 44′ 54.7″ N, 127° 09′ 46.6″ E) was 128 m and its height was 40 m. 6 three-dimensional sonic anemometers (CSAT3, Campbell Scientific Inc., Logan, UT) were installed at 4, 9, 18, 29, 34, and 40 m, respectively. And the elevation of GDK flux tower (37° 45′ N, 127° 09′ E) was 260 m and its height was also 40, but the three-dimensional sonic anemometer was installed only at 40 m.

Table 1. Characteristics of tree of target area

	Conifer tree	**Deciduous tree**
Representative tree type	*Abies holophylla*	*Carpinus* and *Quercus*
Average height (m)	28	20
Average height of trunk (m)	18	10
Leaf area index (LAI) (dimensionless)	4 ~ 8	1 ~ 6

2.2. Computational Fluid Dynamics (CFD)

CFD has been used to solve heat transfer, mass transfer, chemical reaction and other problems in the fields of mechanics, aeronautics and chemical engineering. CFD simulation has also been used in studies of agricultural engineering such as air conditioning, heating, ventilation and wind pressure in greenhouse and livestock buildings (Lee *et al.*, 2004).

CFD numerically solves the Reynolds-averaged form of the Navier-Stokes equations (Launder and Spalding, 1974) within each cell in the computational domain (Lee and Short, 2000). The flows of fluid and energy in CFD are computed using a nonlinear partial differential equation based on the laws of conservation of mass, momentum and energy. A mass conservation equation can be applied to a physical phenomenon irrespective of steady state, viscosity and compressibility. The momentum conservation equation is commonly known as the Navier-Stokes equation. The energy conservation equation indicates a relation of energy exchange in a physical system (Launder and Spalding, 1974). In this study, the commercial CFD package FLUENT (ver. 15.0, ANSYS Inc., PA, USA) was used to compute the governing equation of fluid flow.

2.3. Porosity of trees

In CFD simulation, pressure drop from porous media was calculated by source term in momentum equation. The source term was modelled as a quadratic equation of the velocity magnitude.

$$S_{\Phi} = -(\frac{\mu}{\alpha} v_i + C_2 \frac{1}{2} \rho |v| v_i) \qquad (1)$$

Where, α is the permeability (m^2), μ is the absolute viscosity coefficient (kg s^{-1} m^{-1}), ρ is the

air density (kg m^{-3}), and C_2 is the inertial resistance coefficient (m^{-1}).

In laminar flows through porous media, the pressure drop is typically proportional to velocity and the constant C_2 can be considered to be zero. Therefore, the porous media model reduces to Darcy's Law:

$$\nabla p = -\frac{\mu}{\alpha}\vec{v} \qquad (2)$$

Otherwise, Darcy term can be ignored when the velocity is very fast or Reynolds number (Re) is larger than 5,000. Therefore, the porous media model reduces to Forchheimer term:

$$\nabla p = -C_2\frac{1}{2}\rho|v|v_i \qquad (3)$$

2.4. CFD modelling procedure

3D solid surface model and mesh was designed using numerical digital map of the target area with various pre-processing softwares such as ArcGIS (ver. 10.1, ESRI, CA, USA), AutoCAD (ver. 2014, Autodesk, INC., CA, USA), SketchUp (ver. 7, Google, Ca, USA), Rhinoceros(ver 5, McNeel North America, WA, USA), DesignModeler (ver. 15, ANSYS Inc., CA, USA).

3D complex topography CFD model was designed using contour lines of target area provided from National Geographic Information Institute in South Korea following advanced study (Hong *et al.*, 2011). First, a Triangulated Irregular Network (TIN) structure was created using the "sand box" tool of SketchUp software on the imported the contour map. Second, a solid object was created using the "drape surface over objects" tool of Rhinoceros software on created TIN structure. Finally, the 3D complex topography CFD model was designed using mesh design tool such as DesignModeler, GAMBIT, Tgrid, etc.

Surface of target area was meshed with 15 m triangular grid size considering mesh economy, and diameter of the surface was 4 km. And horizontal mesh was designed with several steps. First, the cell height of bottom layer was 1.0 m from the surface of the 3D CFD model to 30 m. Next cell was design with 1.1 m height and the cell height was increased with 1.1 ratio to 100 m height, and the growth ratio was 1.25 from 100 m to 1.0 km height. And then 6 layers with same height were added over the generated meshes, resulting in a total of 2.0 km in height. The total number of meshes was approximately 5,777,000. The Skewness was generally used to evaluate quality of meshes. The maximum skewnesses of the designed surface and cell mesh were 0.46 and 0.64, respectively, indicating a reasonable mesh quality.

III. Results

3.1. Target site

We calculated pre-vailing wind direction and pre-vailing wind speed using observed wind environmental data of two flux tower from January to December in 2010 to design a boundary condition of simulation model. As a result, the pre-vailing wind speed and direction at GDK tower which is relatively located at west side of Gwangneung Arboretum was observed as 0.5 ~ 1.5 m s^{-1} and WNW direction, respectively. And the pre-vailing wind speed of GCK tower was also observed as 0.5 ~ 1.5 m s^{-1}, but it is hard to set one wind direction as a pre-vailing wind direction because the observed data from the GCK tower shows the similar frequency of every wind direction except east wind to south wind (Fig. 2).

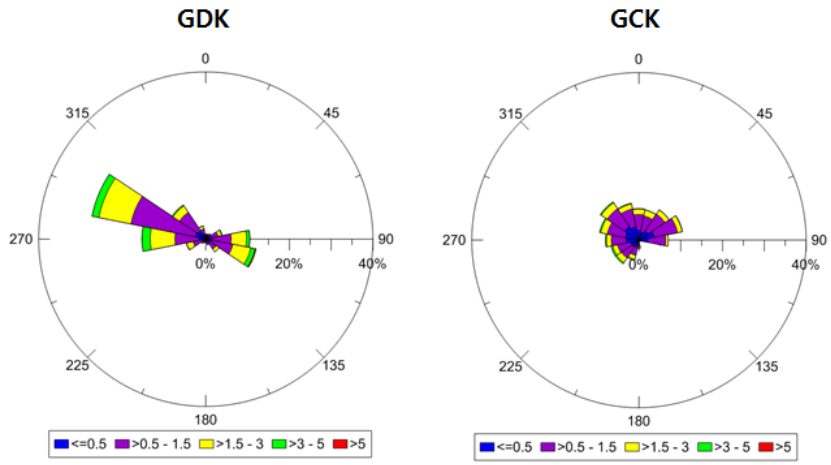

Fig. 2. Results of prevailing wind speed and direction of GDK and GCK towers.

3.2. Target site

The porosity of tree was implemented by development of used defined function (UDF) code, because it is difficult to design separated mesh due to the complex topography and the complex distribution of tree area. The implementation process of the tree porosity by the developed UDF code was following. First, cell wall distance of each cell was calculated and it is saved to user defined memory (UDM) of each cell. And the land use classification database was save to the UDM of each cell based on land use classification data analysed through satellite image or land usage map provided by National geographic information institute (NGII) in South Korea. Finally, the porosity coefficient of tree was implemented by cross analysis of the cell wall distance and land use classification of each cell using conditional statement of developed UDF.

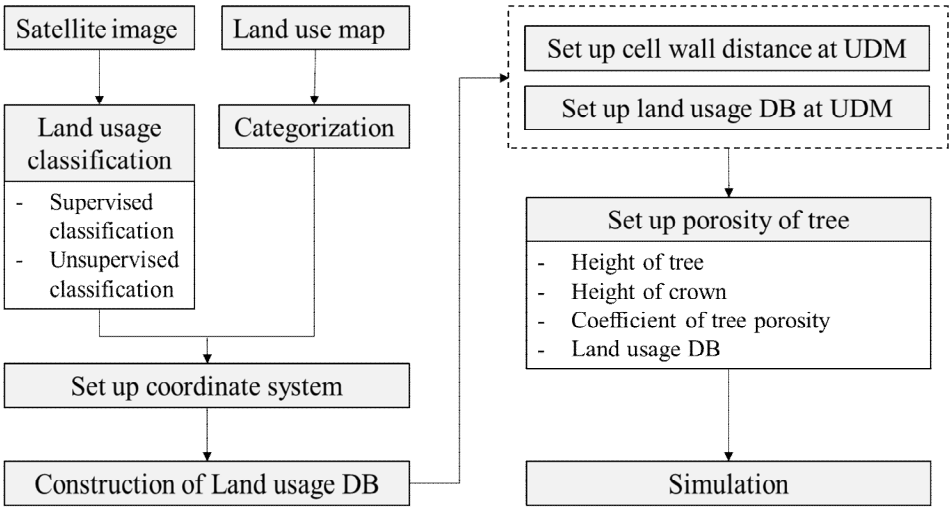

Fig. 3. Flow chart of procedure for implementation of tree porosity to CFD model.

3.3. Validation of CFD simulation model

To validate the significance of CFD simulation model, we compared the simulated data and the 95% confidence interval of observed wind speed and direction of GCK and GDK tower. Specifically, we tried to determine the goodness of turbulence model by testing the simulated data is included to the 95% confidence interval of observed data or not. Specifically, first, we calculated the 95% confidence interval of the observed data from GCK tower and GDK tower under east wind condition. As a result, the confidence interval of wind speed was calculated as 1.23 m/s $\leq WS_{GCK} \leq$ 1.77 m/s from GCK, and 1.51 m/s $\leq WS_{GDK} \leq$ 2.22 m/s from GDK. Also, the confidence interval of wind direction was calculated as 76.7° $\leq WD_{GCK} \leq$ 89.4° from GCK, and 93.0° $\leq WD_{GDK} \leq$ 98.4° from GDK. Second, we deduced the simulated wind speed and direction by using developed CFD simulation model which is calculated using five turbulence model from GCK and GDK tower.

By comparing the observed and simulated result from GCK tower, the simulated data using Standard k-ε and Realizable k-ε turbulence model was included to 95% confidence interval of both wind speed and direction. On the other hand SST k-ω turbulence model shows same result only about wind speed. RNG k-ε and Standard k-ω turbulence model shows no same result. From GDK tower, the simulated data using Standard k-ε turbulence model was included to 95% confidence interval of both wind speed and direction, but the simulated data using rest four models were not included to not only about wind speed but also wind direction.

Table 2. 95% confidence interval fo the observed data from GDK and GCK towers when wind boundary condition was east wind condition

		Average	Standard deviation	Lower limit of C.I.	Upper limit of C.I.	Length of C.I.
GCK	Wind speed (m s^{-1})	1.50	0.53	1.23	1.77	0.54
	Wind direction (degree)	83.1	12.29	76.7	89.4	12.7
GDK	Wind speed (m s^{-1})	1.86	0.69	1.51	2.22	0.71
	Wind direction (degree)	95.7	5.27	93.0	98.4	5.4

Table 3. Simulated results of CFD model according to turbulence models when wind boundary condition was east wind condition

		Standard k-ε	RNG k-ε	Realizable k-ε	Standard k-ω	SST k-ω
GCK	Wind speed (m s^{-1})	82.5	76.4	79.1	94.4	67.3
	Wind direction (degree)	1.72	1.97	1.60	1.14	1.63
GDK	Wind speed (m s^{-1})	93.2	86.3	92.8	87.8	93.2
	Wind direction (degree)	1.65	1.38	1.61	1.16	1.36

We also calculated the 95% confidence interval of the observed data from GCK tower and GDK tower under West wind condition. As a result, the confidence interval of wind speed was calculated as 0.54 m/s ≤ WSGCK ≤ 1.90 m/s from GCK, and 0.37 m/s ≤ WSGDK ≤ 1.25 m/s from GDK. Also, the confidence interval of wind direction was calculated as 263.3° ≤ WDGCK ≤ 286.4° from GCK, and 321.7° ≤ WDGDK ≤ 348.4° from GDK.

By comparing the observed and simulated result from GCK tower, the simulated data using Standard k-ε and Standard k- ω turbulence model was included to 95% confidence interval of both wind speed and direction. On the other hand Realizable k-ε and SST k-ω turbulence model shows same result only about wind direction. Also, the simulated data from GDK tower using Standard k-ε and SST k- ω turbulence model was included to 95% confidence interval of both wind speed and direction. Therefore, we decided the Standard k-ε turbulence model is appropriate to simulate airflow over the complex terrain.

Table 4. 95% confidence interval fo the observed data from GDK and GCK towers when wind boundary condition was east wind condition

		Average	Standard deviation	Lower limit of C.I.	Upper limit of C.I.	Length of C.I.
GCK	Wind speed(m s^{-1})	1.22	0.83	0.54	1.90	1.36
	Wind direction (degree)	274.9	14.13	263.3	286.4	13.1
GDK	Wind speed (m s^{-1})	0.81	0.54	0.37	1.25	0.88
	Wind direction (degree)	335.1	16.40	321.7	348.4	26.7

Table 5. Simulated results of CFD model according to turbulence models when wind boundary condition was east wind condition

		Standard k-ε	RNG k-ε	Realizable k-ε	Standard k-ω	SST k-ω
GCK	Wind speed (m s^{-1})	1.86	2.06	2.00	1.86	2.10
	Wind direction (degree)	264.8	260.5	266.2	266.1	267.7
GDK	Wind speed (m s^{-1})	0.68	0.69	0.73	0.67	0.63
	Wind direction (degree)	346.7	358.8	351.5	348.8	347.6

Acknowledgements

This work was funded by the Weather Information Service Engine Program of the Korea Meteorological Administration under Grant KMIPA-2012-0001.

References

Cheng, X., and F. Hu, 2005: Numerical studies on flow fields around buildings in an urban street canyon and cross-road. *Advances in Atmospheric Sciences* **22**(2), 290-299.

Hong, S., I. Lee, H. Hwang, I. Seo, J. Bitog, K. Kwon, J. Song, O. Moon, K. Kim, and H. Ko, 2011: CFD modelling of livestock odour dispersion over complex terrain, part I: Topographical modelling. *Biosystems Engineering* **108**(3), 253-264. doi:10.1016/j.biosystemseng.2010.12.009

Kim, J. J., and J. J. Baik, 1999: A numerical study of thermal effects on flow and pollutant dispersion in urban street canyons. *Journal of Applied Meteorology* **38**(9), 1249-1261. doi: 10.1175/15 20-0450(1999)038<1249:Ansote>2.0.Co;2

Kim, J. J., and J. J. Baik, 2001: Urban street-canyon flows with bottom heating. *Atmospheric Environment* **35**(20), 3395-3404. doi:Doi 10.1016/S1352-2310(01)00135-2

Launder, B. E., and D. B. Spalding, 1974: The numerical computation of turbulent flows. *Computer methods in applied mechanics and engineering* **3**(2), 269-289.

Lee, I. B., and T. Short, 2000: Two-dimensional numerical simulation of natural ventilation in a multi-span greenhouse. *Transactions of the ASAE* **43**(3), 745-753.

Lee, I. B., B. K. You, C. H. Kang, J. G. Jeun, G. W. Kim, S. H. Sung, and S. Sase, 2004: Study on forced ventilation system of a piglet house. *Japan Agricultural Research Quarterly* **38**(2), 81-90.

Liu, C. H., and M. C. Barth, 2002: Large-eddy simulation of flow and scalar transport in a modeled street canyon. *Journal of Applied Meteorology* **41**(6), 660-673. doi: 10.1175/1520-0450(2002) 041<0660:Lesofa>2.0.Co;2

Sini, J. F., S. Anquetin, and P. G. Mestayer, 1996: Pollutant dispersion and thermal effects in urban street canyons. *Atmospheric Environment* **30**(15), 2659-2677. doi: 10.1016/1352-2310(95)00 321-5

World Meteorological Organization, 1983: *Guide to meteorological instruments and methods of observation*. Secretariat of the World Meteorological Organization.